Biomineralization Hot Paper

DOI: 10.1002/ange.201310712

Functionalizing Single Crystals: Incorporation of Nanoparticles Inside Gel-Grown Calcite Crystals**

*Yujing Liu, Wentao Yuan, Ye Shi, Xiaoqiang Chen, Yong Wang, Hongzheng Chen, and Hanying Li**

Abstract: *Synthetic single crystals are usually homogeneous solids. Biogenic single crystals, however, can incorporate biomacromolecules and become inhomogeneous solids so that their properties are also extrinsically regulated by the incorporated materials. The discrepancy between the properties of synthetic and biogenic single crystals leads to the idea to modify the internal structure of synthetic crystals to achieve nonintrinsic properties by incorporation of foreign material. Intrinsically colorless and diamagnetic calcite single crystals are turned into colored and paramagnetic solids, through incorporation of Au and Fe_3O_4 nanoparticles without significantly disrupting the crystalline lattice of calcite. The crystals incorporate the nanoparticles and gel fibers when grown in agarose gel media containing the nanoparticles, whereas the solution-grown crystals do not. As such, our work extends the long-history gel method for crystallization into a platform to functionalize single-crystalline materials.*

In nature, crystalline materials are widely used by organisms to construct hard tissues.[1–5] Surprisingly, these biogenic materials often exhibit uncommon single-crystal composite structures where biomacromolecules are incorporated inside single-crystalline host, as revealed in the cases of echinoderms (e.g., sea urchins and brittle stars) and mollusk shells (e.g., Atrina rigida and Pinna nobilis).[1,6–14] Intuitively, the incorporated biomacromolecule guest will modify the properties of the single-crystal host and it is believed that the introduction of organic components overcomes the intrinsic brittleness of the single crystals.[15] Thus, the concept of single-crystal composite encourages a principle of material design: modifying and even functionalizing single crystals through incorporation of foreign materials.

Efforts have been made to mimic the biogenic single-crystal composite structures. For example, polymer membranes were used to grow, from solutions, single crystals of calcite with the membranes incorporated;[16,17] similarly, colloidal particles in the presence of the solutions for crystallization can be incorporated into the growing zinc oxide, calcite, and perylene single crystals and metal-organic framework crystals.[18–22] In addition to the solution crystallization, gel-grown calcite crystals were shown to incorporate the three-dimensional (3D) random gel network, resulting in interpenetrating networks of crystals and gel polymers.[23–29] Furthermore, networks with more ordered structures like colloidal crystals[19,30] and gyroid polymer networks[31] have been reported to incorporate into synthetic crystals. Also, foreign materials might be incorporated as, possibly, individual molecules[32–36] instead of their aggregate states. Although single-crystal composites were obtained in many cases,[16–31] the effects of the incorporated materials on the properties of the host crystals are less frequently considered. In a few cases, mechanical properties of the single-crystal composites were investigated.[1,19,37–39] When polymer micelles were incorporated into calcite single crystals, the obtained composites became harder than the "pure" crystals.[38,39] This progress exemplifies the "positive" effect of foreign material incorporation in the sense of mechanical property enhancement. In this work, instead of improving the intrinsic property (e.g., mechanical property) of the crystals, we aim to endow single-crystal hosts with nonintrinsic properties by introducing nanoparticle guest into the crystals. Colorless and diamagnetic calcite single crystals were used as the host materials, while colored Au nanoparticles and paramagnetic Fe_3O_4 nanoparticles were used as guest materials. The most challenging issue of this approach is to promote the crystals to incorporate the nanoparticles but not to push them away during crystal growth. Here, we used gel media to address this issue (Figure 1a). We first dispersed the Au and/or Fe_3O_4 nanoparticles in an agarose hydrogel. Subsequently, calcite crystal growth in the hydrogel-induced incorporation of the gel networks[23] and, also, the nanoparticles trapped in the gel. In this way, we turn intrinsically colorless and diamagnetic calcite single crystals into colored and paramagnetic solids, without substantially disrupting the crystalline lattice.

[*] Y. J. Liu, Y. Shi, X. Q. Chen, Prof. H. Z. Chen, Prof. H. Y. Li
MOE Key Laboratory of Macromolecular Synthesis and Functionalization, State Key Laboratory of Silicon Materials
Department of Polymer Science and Engineering
Zhejiang University, Hangzhou, 310027(China)
E-mail: hanying_li@zju.edu.cn

W. T. Yuan, Prof. Y. Wang
State Key Laboratory of Silicon Materials
Center of Electron Microscopy
Department of Materials Science and Engineering
Zhejiang University, Hangzhou, 310027 (China)

[**] This work was supported by the National Natural Science Foundation of China (grant numbers 51222302, 51373150,50990063, 51261130582, and 91233114), Major State Basic Research Development Program (grant number 2014CB643503), Zhejiang Province Natural Science Foundation (grant number LZ13E030002), Scientific Research Foundation for the returned overseas chinese scholars, State Education Ministry, and Fundamental Research Funds for the Central Universities.

Supporting information for this article including the complete details of the synthesis of the Au and Fe_3O_4 nanoparticles, preparation of the gel, crystallization, and analytical methods is available on the WWW under http://dx.doi.org/10.1002/anie.201310712.

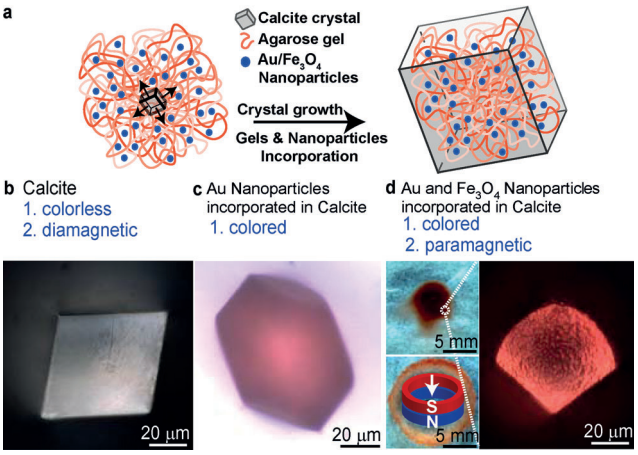

Figure 1. a) Crystallization in gel media containing dispersed nanoparticles. b) Optical microscopy (OM) image of the colorless and diamagnetic calcite crystals grown in an agarose gel (0.5 w/v%, agarose IB). c) OM image of the colored calcite crystals grown in an agarose gel containing Au nanoparticles (0.5 w/v%, agarose IB; 8 mg mL^{-1}, 20 nm Au nanoparticles). d) OM image of the colored and paramagnetic calcite crystals grown in an agarose gel containing both Au and Fe_3O_4 nanoparticles (0.5 w/v%, agarose IB; 3 mg mL^{-1}, 20 nm Au nanoparticles; 2 mg mL^{-1}, 5 nm Fe_3O_4 nanoparticles). The two photos on the left record how the crystals moved outward in a magnetic field, which is also shown in movie S1 in the Supporting Information.

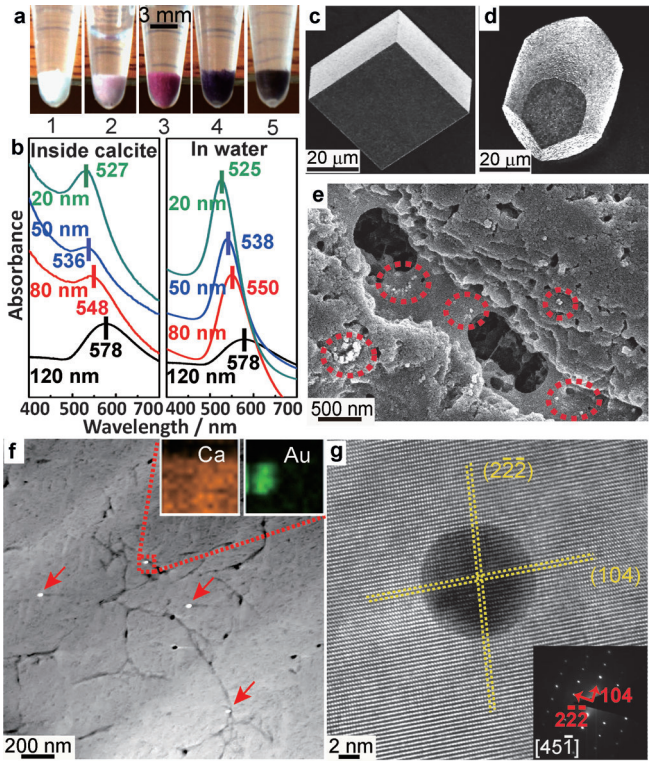

Figure 2. a) Photos of crystals grown in an agarose gel (0.5 w/v%, agarose IB) containing Au nanoparticles of varied concentrations and sizes: 1) without nanoparticles; 2) 0.5 mg mL^{-1}, 20 nm; 3) 2 mg mL^{-1}, 20 nm; 4) 4 mg mL^{-1}, 20 nm; 5) 4 mg mL^{-1}, 80 nm. b) UV/Vis diffuse reflectance spectra of crystals grown in an agarose gel (0.5 w/v%, agarose IB) containing Au nanoparticles of varied sizes (1 mg mL^{-1}, 20–120 nm, left panel) and UV/Vis absorption spectra of Au nanoparticles dispersed in water (20–80 nm: 2 mg mL^{-1}, 120 nm: 1 mg mL^{-1}, right panel). c–e) Representative SEM images of calcite crystals grown in an agarose gel containing Au nanoparticles: c) as grown at low Au nanoparticles concentration (0.5 w/v%, Agarose IB; 0.5 mg mL^{-1}, 20 nm Au nanoparticles); d) as grown at high Au nanoparticles concentration (0.5 w/v%, Agarose IB; 8 mg mL^{-1}, 20 nm Au nanoparticles); e) etched crystals grown at high Au nanoparticle concentration (0.5 w/v%, Agarose IB; 8 mg mL^{-1}, 20 nm Au nanoparticles). The Au nanoparticles exposed in the etch pits are highlighted by red dotted circles. f) A HAADF-STEM image of a thin section cut from the calcite crystal grown in an agarose gel containing Au nanoparticles (highlighted by red arrows) (0.5 w/v%, Agarose IB; 1 mg mL^{-1}, 20 nm Au nanoparticles). Inset: EDX maps of the highlighted area where the bright dots are identified as Au. g) A HRTEM image showing the lattice fringes around a Au nanoparticle. Inset: A SAED pattern of a region (3 μm in diameter) containing crystal host, gel fibers, and Au nanoparticles.

Calcite crystals were grown, in agarose hydrogels (agarose IB, 5 mM $CaCl_2$), using the previously reported ammonium carbonate method.[25,40] Rhombohedral single crystals of calcite incorporating a gel network[23] (Figure 1b and Figure S1 in the Supporting Information) were obtained, showing no color. As Au nanoparticles[41] (0.5 mg mL^{-1}, 20 nm, coated with poly(vinylpyrrolidone) (PVP) to prevent aggregation; Figure S2a) were dispersed in the hydrogels before crystallization, the subsequently grown calcite maintained the characteristic rhombohedral morphology but became colored. With the increase of Au nanoparticle concentration (0.5–8 mg mL^{-1}) in the hydrogels, the sharp crystal edges (Figure 2c) gradually evolved to curved surfaces (Figure 1c and d) and the color turned darker (Figure 2a and Figure S3). The shape evolution is probably associated with the interactions between crystal (possibly in a direction perpendicular to the *ab* plane) and Au (and/or PVP) as well as agarose that affect the growth kinetics anisotropically, similar to the effects of varied additives.[1,42–44] In addition to the increase of Au nanoparticle concentration, the color of the crystals can also be tuned from red to violet by using Au nanoparticles with increasing sizes (20–120 nm; Figure 2a,b).

The color of the crystals indicated that the crystals were decorated with Au nanoparticles. UV/Vis diffuse reflectance spectroscopy (DRS) of the colored crystals showed similar absorption peaks as those of the Au nanoparticles dispersed in water (Figure 2b), confirming the association of the nanoparticles with the crystals. As the nanoparticles on the surface of the crystals were removed by ultrasonication (6 h in water), the color was expected to originate from the Au nanoparticles inside the bulk. To elucidate if the nanoparticles were absorbed on the surface or incorporated inside the crystals, we imaged, by scanning electron microscopy (SEM), the crystals before and after gentle etching. Before etching, a few nanoparticles on the surfaces were observed (Figure 2c). After etching, the nanoparticles were exposed in the etch pits (Figure 2e). The SEM images preliminarily indicated that the nanoparticles were incorporated inside the crystals, which was reconfirmed by high-angle annular-dark-field scanning transmission electron microscopy (HAADF-STEM). HAADF-STEM images of a thin section of the crystal revealed the gel fibers inside the crystal, similar to those of the previously

reported gel-grown crystals.[23] In between the fibers, bright dots of nanoparticles were also observed, which were assigned as Au nanoparticles by energy-dispersive X-ray spectroscopy (EDX; Figure 2f). More interestingly, high-resolution transmission electron microscopy (HRTEM) showed 2D lattice images where lattice fringes translated across the nanoparticles (Figure 2g), indicating that the incorporation of the nanoparticles did not break the long-range order of the host crystals. Also, selected-area electron diffraction (SAED) of a large area (3 μm in diameter), including Au nanoparticles and gel fibers, showed a single set of diffraction spots of calcite, indicative of the single-crystallinity of the calcite (Figure 2g). Therefore, the SEM, HAADF-STEM, and TEM images and the selected-area electron diffractograms demonstrate that we have obtained calcite single crystals incorporating Au nanoparticles and agarose gel fibers, and the optical microscopy images and the UV/Vis diffuse reflectance spectra prove that the incorporation of the nanoparticles leads to a color characteristic, a nonintrinsic optical property of the host calcite crystals.

Besides the optical property, we also investigated the possibility to endow the calcite single crystal with a magnetic property by functionalization. Similarly, the paramagnetic Fe_3O_4 nanoparticles[45] (Figure S2b) were dispersed in the hydrogels where the calcite crystals grew subsequently. The crystals as grown retain the characteristic rhombohedral morphology (Figure 3a). Interestingly, the crystals became paramagnetic and moved around, driven by a magnetic field (Figure 3a,b). SEM images and EDX analysis of the gently etched crystals revealed the incorporated Fe_3O_4 nanoparticles (Figure 3c). Both SAED and HRTEM lattice images demonstrated that even in the presence of gel fibers and nanoparticles, the crystals still retained their single-crystal nature (Figure 3d). Therefore, we achieved the paramagnetism in the intrinsic diamagnetic calcite single crystals, through nanoparticle incorporation. Furthermore, both Au and Fe_3O_4 nanoparticles were incorporated simultaneously into the crystals to achieve multi-functionalization of calcite single crystals (Figure 1d and Movie S1).

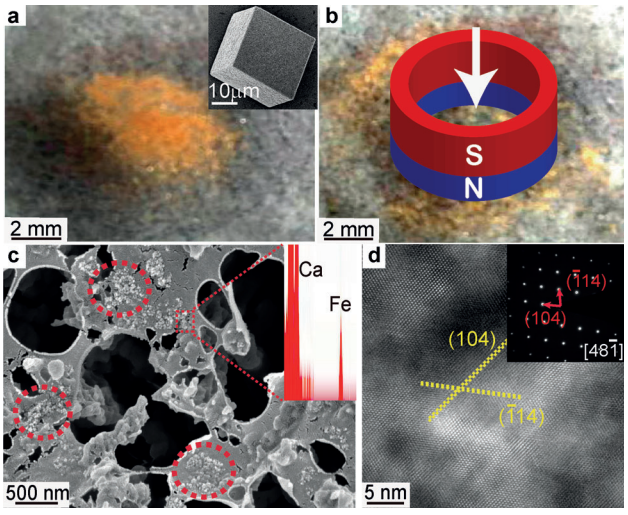

Figure 3. a,b) Photos of the crystals, showing how they moved outward in a magnetic field. The inset in (a) shows a SEM image of a calcite crystal grown in an agarose gel containing Fe_3O_4 nanoparticles. c) A SEM image of an etched crystal. Red dotted circles highlight the nanoparticles exposed in the etch pits that are identified by EDX (Inset). d) A HRTEM lattice image of a thin section cut from a crystal. Inset: A SAED pattern of a region (3 μm in diameter).

After proving the approach of functionalizing calcite single crystals, we proceeded to elucidate the mechanism of nanoparticle incorporation, especially the function of the hydrogel media. We examined the calcite crystals grown from hydrogels with increasing gel concentrations, different gel types, and varied sizes of Au nanoparticles.

First, we investigated the effect of gel concentration on the nanoparticle incorporation. When solution growth was used instead of hydrogels, the crystals obtained were almost colorless, shown by UV/Vis spectroscopy, even if the Au concentration was increased to eight times higher than that used in the gel method (Figure 4a). The TEM image showed that there were almost no Au nanoparticles incorporated inside the solution-grown crystals (Figure S4). The UV/Vis and TEM results suggest that the growing crystals did not incorporate the nanoparticles in the solution but pushed them to accumulate on the crystal surfaces (Figure 4b), which was reconfirmed by the following SEM evidences. To examine the nanoparticles absorbed on the crystal surfaces, the as-grown crystals were imaged without sonication. Clearly, a large amount of nanoparticles was observed (Figure 4c). Further, as we increased the gel concentration from 0.1 to 3 w/v% at a fixed nanoparticle concentration (1 mg mL^{-1}), the amount of Au nanoparticles adhered on the crystal surfaces decreased gradually (Figure 4d–h). The discrepancy between crystals grown from solutions and gels indicates that agarose gel media is necessary to induce the nanoparticle incorporation. Interestingly, the solution-grown crystals in the presence of Au nanoparticles remained rhombohedral in morphology (Figure 4c). Also, the gel-incorporated crystals (without the Au nanoparticles) were expressed as rhombohedron (Figure 1b and S1a) as previously reported.[23] In contrast, the morphology changed only when both gel and Au nanoparticles were incorporated (Figure 4 and Figure S5), suggesting a synergic morphological effect of the agarose fibers and the nanoparticles.

Second, the effect of different agarose types on nanoparticle incorporation was examined. Previously, calcite crystals grown from agarose (type IB, used in this work) gels were found to incorporate the gel networks,[23] whereas those grown from another type of agarose gels (type IX, partially hydroxyethylated) that are mechanically weaker did not incorporate the gel networks under specific conditions because the weak gel-network could not sustain the crystallization pressure.[26,46] As described above (Figure 2), the crystals grown from agarose IB gel incorporated both the gel polymers and nanoparticles. However, as the crystals were grown from agarose IX gel (0.8 w/v%) containing Au nanoparticles (1 mg mL^{-1}), almost no particles were incorporated, similar to those grown from solution (Figure 4a). The discrepancy between the two types of agarose gels indicates that gel incorporation is the prerequisite for the nanoparticles to be incorporated.

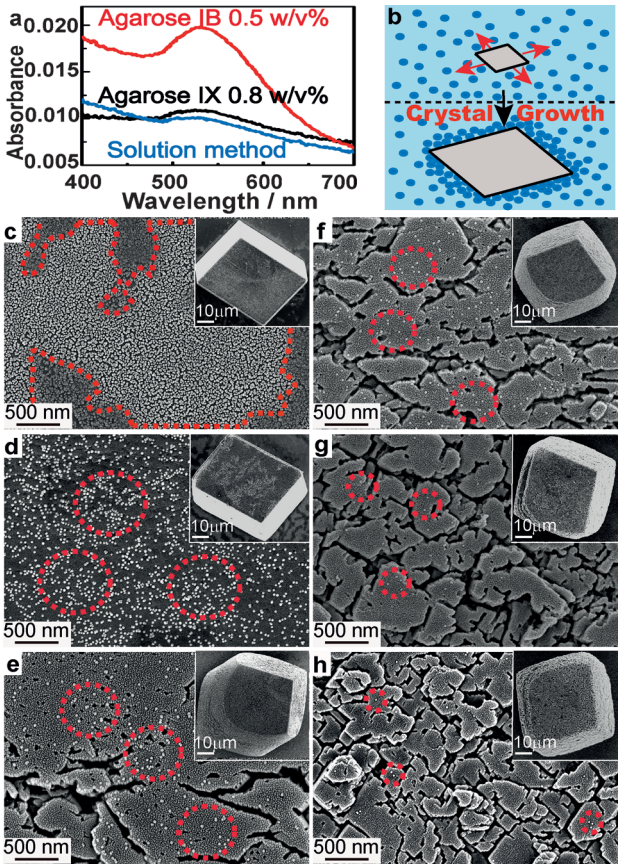

Figure 4. a) UV/Vis absorption spectra of the Au nanoparticles incorporated inside calcite crystals grown from solution (containing 8 mg mL^{-1}, 20 nm Au nanoparticles) or gels (agarose IB, 0.5 w/v% or agarose IX, 0.8 w/v% containing 1 mg mL^{-1}, 20 nm Au nanoparticles). The Au nanoparticles were released from the crystals into aqueous solutions by dissolving 10 mg crystals in 1 mL dilute hydrochloric acid. UV/Vis absorption spectra of the aqueous solutions were measured; b) Schematic diagram of the crystallization in solutions where a growing crystal pushes the Au nanoparticles to accumulate on the crystal surfaces. c–h) SEM images of Au nanoparticles absorbed on the surfaces of the crystals grown in solution or agarose IB gels with varied gel concentrations: c) solution; d) 0.1 w/v% gel; e) 0.5 w/v% gel; f) 1 w/v% gel; g) 2 w/v% gel; h) 3 w/v% gel. The irregularly grooved surfaces are due to the gentle etching by hot water when the crystals were removed from the gels. To examine the nanoparticles absorbed on the crystal surfaces, the as-grown crystals were imaged without sonication. Red dotted lines or circles highlight parts of the Au nanoparticles on the crystal surfaces. Insets: images at low magnification.

Finally, we increased the size of the Au nanoparticles at a fixed molarity of the nanoparticles of 0.2 μM (20 nm: 1 mg mL^{-1}; 50 nm: 15.625 mg mL^{-1}; 80 nm: 64 mg mL^{-1}; 120 nm: 216 mg mL^{-1}), and also the gel concentration (0.5 w/v%), to study the effect of the nanoparticle size. Similarly, the as-grown crystals were imaged without sonication to observe the nanoparticles absorbed on the crystal surfaces. With the increased nanoparticle size, less and less nanoparticles were found on the crystal surfaces (Figure S6). The effect of nanoparticle size on the nanoparticle incorporation suggests that the larger nanoparticles in the gels tend to be incorporated.

Based on the above observations, we propose a mechanism by which nanoparticles are incorporated. 1) The growing crystals tend to push away the nanoparticles. And we observed nanoparticles accumulated on the surfaces of the solution-grown crystal. 2) The gel networks reduce the diffusivity of the nanoparticles that are, therefore, trapped in the network. Larger nanoparticles are easier to be trapped for a given network pore size. 3) The growing crystals incorporate the gel network and also the trapped nanoparticles. We observed that nanoparticles were incorporated only if the gel polymers were incorporated. Assuming that growing crystals incorporate all the nanoparticles they encounter when grown in agarose IB gels with high gel concentrations (e.g., 2 w/v%) and the Au concentration in the gels is about 64 mg mL^{-1}, the concentration of the nanoparticles guest in the crystal host is about 2.4 w/w%.

In summary, we have used Au nanoparticles to "dye" the calcite single crystals[33] and Fe_3O_4 nanoparticles to endow the crystals with paramagnetism. The optical and magnetic functionalizations are achieved through nanoparticle incorporation inside the single crystals. Gel growth media instead of solutions are necessary to induce the incorporation of nanoparticles during which crystals incorporate the gel network and also the nanoparticles trapped in the gels. In contrast to other mechanisms of particle incorporation that are associated with fast crystallization and/or crystal-particle mutual wetting,[47] the gel-mediating strategy described here allows a wide range of particles to be incorporated. We notice that, very recently, this strategy has been used to prepared calcite single crystals with incorporated ZnO and Fe_3O_4 nanoparticles.[48] This work creates a novel and facile pathway to design functionalized single-crystalline materials to expand their potential applications.

Experimental Section

Please see the Supporting Information for complete details of the synthesis of Au and Fe_3O_4 nanoparticles, gel preparation, crystallization and analytical methods.

Received: December 10, 2013
Published online: March 12, 2014

Keywords: biomineralization · functionalization · hydrogels · nanoparticles · single crystals

[1] *Biomineralization*, *Vol. 54* (Eds.: P. M. Dove, J. J. DeYoreo, S. Weiner), The Mineralogical Society of America, Washington, DC, USA, **2003**.
[2] L. Kabalah-Amitai, B. Mayzel, Y. Kauffmann, A. N. Fitch, L. Bloch, P. U. P. A. Gilbert, B. Pokroy, *Science* **2013**, *340*, 454.
[3] L. M. Gordon, D. Joester, *Nature* **2011**, *469*, 194.
[4] A. Veis, *Science* **2005**, *307*, 1419.
[5] F. Nudelman, N. A. J. M. Sommerdijk, *Angew. Chem.* **2012**, *124*, 6686; *Angew. Chem. Int. Ed.* **2012**, *51*, 6582.
[6] Y. Politi, T. Arad, E. Klein, S. Weiner, L. Addadi, *Science* **2004**, *306*, 1161.
[7] J. Aizenberg, A. Tkachenko, S. Weiner, L. Addadi, G. Hendler, *Nature* **2001**, *412*, 819.

[8] F. Nudelman, H. H. Chen, H. A. Goldberg, S. Weiner, L. Addadi, *Faraday Discuss.* **2007**, *136*, 9.
[9] J. Aizenberg, J. Hanson, T. F. Koetzle, S. Weiner, L. Addadi, *J. Am. Chem. Soc.* **1997**, *119*, 881.
[10] A. Berman, J. Hanson, L. Leiserowitz, T. F. Koetzle, S. Weiner, L. Addadi, *Science* **1993**, *259*, 776.
[11] H. Y. Li, H. L. Xin, M. E. Kunitake, E. C. Keene, D. A. Muller, L. A. Estroff, *Adv. Funct. Mater.* **2011**, *21*, 2028.
[12] K. Gries, R. Kroger, C. Kubel, M. Fritz, A. Rosenauer, *Acta Biomater.* **2009**, *5*, 3038.
[13] J. S. Robach, S. R. Stock, A. Veis, *J. Struct. Biol.* **2005**, *151*, 18.
[14] Y. Dauphin, *J. Biol. Chem.* **2003**, *278*, 15168.
[15] L. Addadi, S. Weiner, *Angew. Chem.* **1992**, *104*, 159; *Angew. Chem. Int. Ed. Engl.* **1992**, *31*, 153.
[16] R. J. Park, F. C. Meldrum, *J. Mater. Chem.* **2004**, *14*, 2291.
[17] R. J. Park, F. C. Meldrum, *Adv. Mater.* **2002**, *14*, 1167.
[18] R. Muñoz-Espí, A. Chandra, G. Wegner, *Cryst. Growth Des.* **2007**, *7*, 1584.
[19] Y. Y. Kim, L. Ribeiro, F. Maillot, O. Ward, S. J. Eichhorn, F. C. Meldrum, *Adv. Mater.* **2010**, *22*, 2082.
[20] C. Li, L. M. Qi, *Angew. Chem.* **2008**, *120*, 2422; *Angew. Chem. Int. Ed.* **2008**, *47*, 2388.
[21] M. Sindoro, Y. Feng, S. Xing, H. Li, J. Xu, H. Hu, C. Liu, Y. Wang, H. Zhang, Z. Shen, H. Chen, *Angew. Chem.* **2011**, *123*, 10072; *Angew. Chem. Int. Ed.* **2011**, *50*, 9898.
[22] G. Lu, S. Li, Z. Guo, O. K. Farha, B. G. Hauser, X. Qi, Y. Wang, X. Wang, S. Han, X. Liu, J. S. DuChene, H. Zhang, Q. Zhang, X. Chen, J. Ma, S. C. J. Loo, W. D. Wei, Y. Yang, J. T. Hupp, F. Huo, *Nat. Chem.* **2012**, *4*, 310.
[23] H. Y. Li, H. L. Xin, D. A. Muller, L. A. Estroff, *Science* **2009**, *326*, 1244.
[24] H. Y. Li, L. A. Estroff, *CrystEngComm* **2007**, *9*, 1153.
[25] H. Y. Li, L. A. Estroff, *J. Am. Chem. Soc.* **2007**, *129*, 5480.
[26] H. Y. Li, L. A. Estroff, *Adv. Mater.* **2009**, *21*, 470.
[27] O. Grassmann, R. B. Neder, A. Putnis, P. Lobmann, *Am. Mineral.* **2003**, *88*, 647.
[28] H. J. Nickl, H. K. Henisch, *J. Electrochem. Soc.* **1969**, *116*, 1258.
[29] Y. Oaki, S. Hayashi, H. Imai, *Chem. Commun.* **2007**, 2841.
[30] E. J. W. Crossland, N. Noel, V. Sivaram, T. Leijtens, J. A. Alexander-Webber, H. J. Snaith, *Nature* **2013**, *495*, 215.
[31] A. S. Finnemore, M. R. J. Scherer, R. Langford, S. Mahajan, S. Ludwigs, F. C. Meldrum, U. Steiner, *Adv. Mater.* **2009**, *21*, 3928.
[32] R. A. Metzler, G. A. Tribello, M. Parrinello, P. Gilbert, *J. Am. Chem. Soc.* **2010**, *132*, 11585.
[33] B. Kahr, R. W. Gurney, *Chem. Rev.* **2001**, *101*, 893.
[34] A. W. Xu, M. Antonietti, S. H. Yu, H. Colfen, *Adv. Mater.* **2008**, *20*, 1333.
[35] H. Cölfen, S. Mann, *Angew. Chem.* **2003**, *115*, 2452; *Angew. Chem. Int. Ed.* **2003**, *42*, 2350.
[36] S. Borukhin, L. Bloch, T. Radlauer, A. H. Hill, A. N. Fitch, B. Pokroy, *Adv. Funct. Mater.* **2012**, *22*, 4216.
[37] J. M. García-Ruiz, J. A. Gavira, F. Otálora, A. Guasch, M. Coll, *Mater. Res. Bull.* **1998**, *33*, 1593.
[38] Y. Y. Kim, K. Ganesan, P. C. Yang, A. N. Kulak, S. Borukhin, S. Pechook, L. Ribeiro, R. Kroger, S. J. Eichhorn, S. P. Armes, B. Pokroy, F. C. Meldrum, *Nat. Mater.* **2011**, *10*, 890.
[39] L. A. Estroff, I. Cohen, *Nat. Mater.* **2011**, *10*, 810.
[40] J. Aizenberg, A. J. Black, G. M. Whitesides, *J. Am. Chem. Soc.* **1999**, *121*, 4500.
[41] S. D. Perrault, W. C. W. Chan, *J. Am. Chem. Soc.* **2009**, *131*, 17042.
[42] J. J. De Yoreo, P. M. Dove, *Science* **2004**, *306*, 1301.
[43] K. J. Davis, P. M. Dove, L. E. Wasylenki, J. J. De Yoreo, *Am. Mineral.* **2004**, *89*, 714.
[44] C. A. Orme, A. Noy, A. Wierzbicki, M. T. McBride, M. Grantham, H. H. Teng, P. M. Dove, J. J. DeYoreo, *Nature* **2001**, *411*, 775.
[45] S. Xuan, L. Hao, W. Jiang, X. Gong, Y. Hu, Z. Chen, *J. Magn. Magn. Mater.* **2007**, *308*, 210.
[46] E. Asenath-Smith, H. Y. Li, E. C. Keene, Z. W. Seh, L. A. Estroff, *Adv. Funct. Mater.* **2012**, *22*, 2891.
[47] A. A. Chernov, *Modern Crystallography III: Crystal Growth*, *Vol. 36*, Springer, New York, **1984**.
[48] Y. Y. Kim, A. S. Schenk, D. Walsh, A. N. Kulak, O. Cespedes, F. C. Meldrum, *Nanoscale* **2014**, *6*, 852.

